

Chapter 2

Polarization Error Compensation in Dual-Polarization IFOGs

In this chapter, two kinds of dual-polarization IFOGs are designed and experimentally tested, and the phenomenon of polarization nonreciprocity (PN) error compensation between two polarizations is observed. The experimental structures ensure that two polarizations are independent for rotation sensing. The two polarization states undergo polarizing, splitting, traveling through the fiber loop, and interfering, respectively. As the two optical waves are subjected to the same fiber loop, there is unavoidable coupling. Hence, the error components in two detection signals are correlated. Experimental results show that a large part of the error components between two signals are just opposite. It is then proved that this part of error is the PN error introduced by polarization coupling. A mathematical model is established for analyzing the dual-polarization PN error compensation. A conclusion has been arrived that the PN errors in dual-polarization IFOGs can be compensated by superimposition.

2.1 First Observation of Polarization Error Compensation in an IFOG

Optical fiber supports the propagation of two orthogonal polarization modes, so sensing with two polarizations is the natural potential of IFOG. Similar to the polarization multiplexing in the field of optical fiber communication, in the field of optical sensing, the simultaneous use of two polarization states will bring additional signal, also bring new features. In the previous chapter, some relevant studies of dual-polarization IFOGs are reviewed. These studies exploit the features of two orthogonal polarization modes available in the fiber and achieve different objectives in the IFOG. However, the potential of dual-polarization IFOG is not limited to this, and the law of the evolution of two polarization states in IFOG is still not clear. Therefore, dual-polarization IFOG needs further investigation.

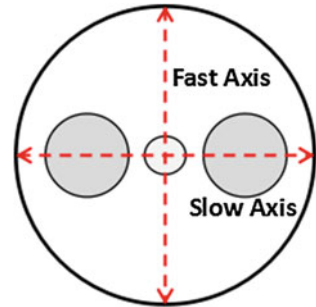
In 2012, the research work of our group aims to improve the performance of a polarization-maintaining IFOG (PM-IFOG) by using two polarization states [1]. In polarization-maintaining fiber (PMF), there are two orthogonal polarization states, as shown in Fig. 2.1. Two polarization states can propagate relatively independently in the PMF, so it can be considered that there are two rotation sensing channels in the IFOG.

The conventional PM-IFOG suppresses one of the polarization modes by using a polarizer and several polarization-maintaining devices, and utilizes the other polarization mode for rotation sensing. Using slow axis for instance, the light wave in the entire fiber loop is in the slow axis polarization state. In the nonideal case, PN errors arise if light component of the slow axis leaks to the fast axis. The function of the polarizer is to reduce the PN error as much as possible. Considering such a single-polarization operation way is a waste of fiber capacity, we have designed a scheme that allows two polarizations working and detecting simultaneously. The experimental structure of the IFOG involved in this design is shown in Fig. 2.2.

In the IFOG experimental setup, a 1550 nm amplified spontaneous emission (ASE) light source with a spectral width of 40 nm was used, and the polarization of the output light was approximately depolarized. Light wave was divided into two beams with equal power after the source coupler, forming two arms of optical paths. There was a 2 m delay line between the two arms (i.e., the fiber length difference between the two arms is 2 m) to ensure that the two light beams are not coherent after entering the fiber loop. One of the two arms had an adjustable attenuator as a power controller, for adjusting the optical power balance. The two beams were respectively polarized, split, and subjected to phase modulation at a Y-junction waveguide. The light beams split by the Y-junction waveguide were cross-connected to two polarization splitters/combiners (PBS/C) as shown in Fig. 2.2. One of the two beams had a polarization rotation by 90° , which realized that two orthogonal polarization modes propagated in the same PMF coil in both CW and CCW directions. The total length of the fiber coil was 1970 m and its radius was 5 cm. The extinction ratio of the Y-junction waveguide was about 35 dB, and a 40 kHz sinusoidal signal was used for phase modulation.

When the dual-polarization light went out from the coil, it would return back to its original light paths, and be reassigned into the two arms. Finally, two

Fig. 2.1 Two orthogonal polarization states in the Panda-type PMF



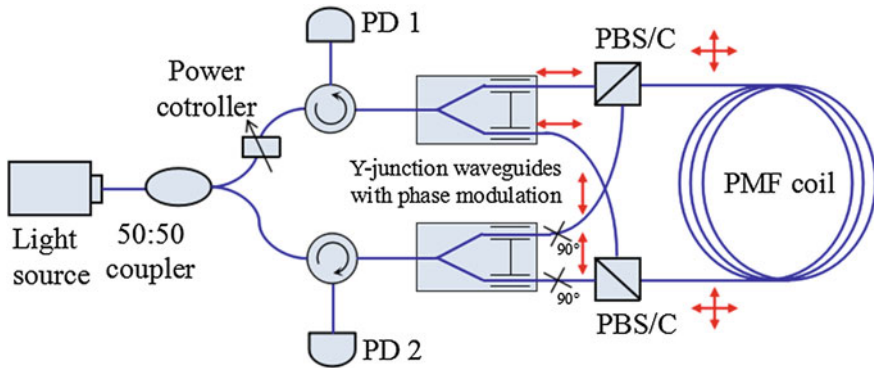


Fig. 2.2 A dual-polarization IFOG based on polarization-maintaining circuit

interference signals were detected by two photoelectric detectors (PD) after passing through the optical circulators. The detection signals were collected by a digital acquisition card (NI PXI 5922) and then processed in a computer by digital signal processing (DSP). In the experiment, the two polarization states of x and y were phase modulated by the same sinusoidal signal and the Sagnac phase shift is obtained by demodulation with 1, 2, and 4 harmonics [2]. In order to verify the compensation effect, two signals were directly summed up to produce the third signal while DSP. Totally three signals were demodulated and thus arrived at three angular velocity outputs.

In the experimental test, the optical structure was placed horizontally on an optical platform, in a stationary state relative to the Earth. Therefore, the Earth's rotation was the only detected rotation signal. The laboratory latitude was 39.99° N, and the projection of the Earth's rotation angular velocity on the horizontal plane was $9.667^\circ/\text{h}$. The sampling interval of the IFOG was 0.15 s. A group of data within 50 min were collected and analyzed. The experimental results are shown in Fig. 2.3. Obviously, errors on the two single-polarization outputs were relatively large. There were fluctuations and glitches in the output of the time domain signal, as shown in the curves "Single axis 1" and "Single axis 2." As a clear comparison, the signal after the superimposition was much more stable, as shown in the "Compensated Output" curve.

This experiment shows that a simple superimposition of two detection signals can reduce the noise in the IFOG. In order to show the improvement of noise parameters more clearly, Allan variance analysis is applied [3, 4], results of which are shown in Fig. 2.4. It can be seen that the whole noise curve of the compensated result is lower than the results of the two polarization states alone, indicating that both short-term noise and long-term drift are significantly reduced. The bias drift is reduced from $0.335^\circ/\text{h}$ and $0.227^\circ/\text{h}$ (for two single-polarization signals respectively) to $0.061^\circ/\text{h}$.

These experimental results show that the noise components in two polarizations can be compensated by summing up the light intensities, thereby reducing the error

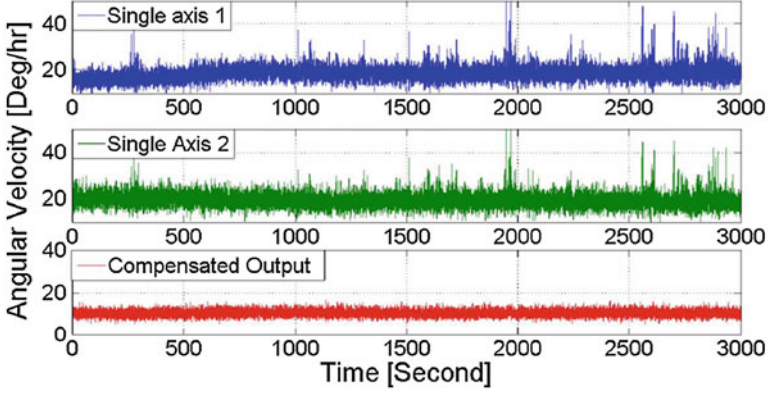


Fig. 2.3 Angular velocity output of the dual-polarization IFOG [1]. (Reprinted from Ref. [1], with kind permission from the Optical Society)

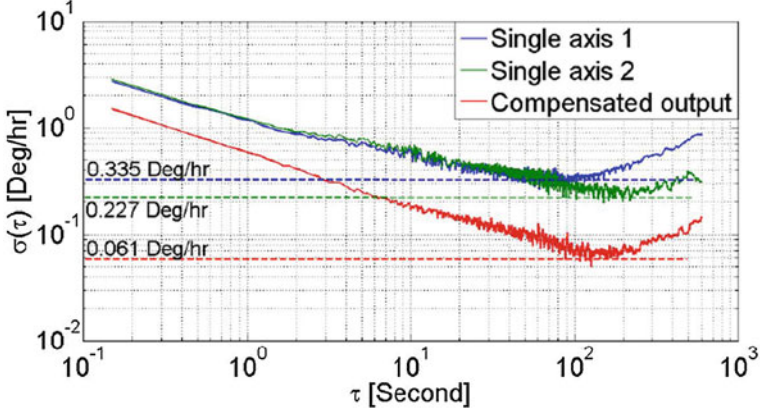


Fig. 2.4 Allan variance analysis of the dual-polarization IFOG [1]. (Reprinted from Ref. [1], with kind permission from the Optical Society)

in the detection results. In general, the polarization error present in IFOG can be divided into intensity error and amplitude error [2]. Preliminary analysis shows that both the intensity error and the amplitude error in the dual-polarization IFOG are with opposite signs between two polarizations. That is to say, the polarization errors in two detected signals are complementary and can be eliminated by superimposition.

Polarization coupling in PMF coil is relatively small, so the PN errors in two detection results are relatively small too. Although the two signal superimposition result shows the compensation effectiveness of PN noises, but the signal characteristics of opposite signs is still not clear to be seen directly. In order to observe the phenomenon of PN error compensation more clearly, we have designed a

dual-polarization IFOG structure with a depolarized fiber coil. The polarization coupling in the depolarized coil is strong, and the PN error can be observed clearly in time domain when the two polarizations are detected separately, and it is more convenient for us to observe the regular pattern.

2.2 Polarization Error Compensation in an Depolarized IFOG

In order to observe and verify the polarization error compensation phenomenon in the IFOG with the depolarized fiber loop, we designed a polarization splitting structure shown in Fig. 2.5. The optical fiber coil is mainly built with common single-mode optical fiber. Two depolarizers are used to eliminate the coherence of the PN light component and a piezoelectric transducer (PZT) is used for phase modulation. The design principle of this fiber coil is consistent with the traditional depolarized IFOG based on the “minimal scheme.”

This structure differs from the conventional depolarized IFOG in that the light entering the coil is in a dual-polarization state. The part of the dotted line in the optical path is the module that generates the dual-polarization light, and detection results of the two polarizations can be observed at the same time. A PBS/C was used for polarization splitting (PBS 1 in the figure), and a 2 m fiber delay line was inserted in one of the two arms for decoherence. Then two light beams were recombined by a second PBS/C (PBS 2), forming a dual-polarization light beam. The dual-polarization light beam was split by an ordinary single-mode coupler to form CW and CCW light waves into the fiber coil. Following the light source, a depolarizer (Depolarizer 1) was used to ensure that the two single-polarization beams after PBS1 were balanced in power. In this way, double-polarization light was generated after PBS2, with power-balanced and incoherent light components between x and y polarizations.

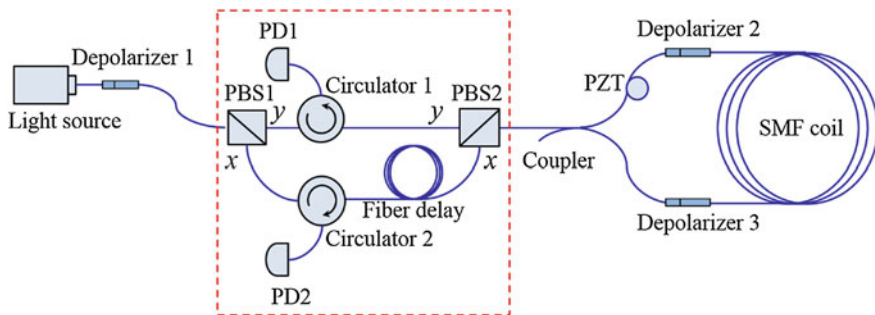
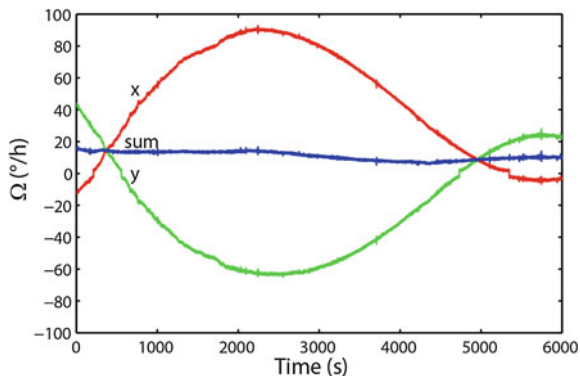


Fig. 2.5 A dual-polarization IFOG based on a depolarized fiber coil

Fig. 2.6 Polarization error compensation in the depolarized IFOG



In the experiment, an ASE light source with a center wavelength of 1550 nm and a spectral width of 40 nm was used, and a 2097 m SMF coil was used. The test goal was still the Earth's rotation rate (9.667 °/h projected at the laboratory latitude). Similar to the previous section, digital signal processing methods were used for angular velocity demodulation from x , y signals and the sum of the two. The experimental results are shown in Fig. 2.6.

Through the test results of this structure, the polarization error compensation can be clearly observed. Polarization coupling is a small amount for PMF coils, but it is larger in a depolarized fiber coil. Therefore, the PN error introduced by random polarization coupling is obvious in both polarization states, leading to significant ripples in the single-channel angular velocity detection results. At the same time, the PN errors of the signal detected by the two polarizations are inverse numbers, so the complementary features can be seen clearly on the graph. The process of summing up the two signals can cancel most PN errors.

The purpose of this experimental structure is to observe the internal mechanism of polarization error compensation. The compensation condition is not the best, so the compensated signal still has some fluctuations, which infers a small part of PN error is left. More practical polarization error compensation IFOG structures are discussed in the next chapter.

2.3 Theoretical Analysis of Polarization Error Compensation

Polarization error compensation is observed and verified in both the dual-polarization IFOG with a PMF coil and the dual-polarization IFOG with a depolarized fiber coil. But it still needs rigorous theoretical analysis for why the two signals have the complementary error and under what conditions can achieve the best compensation effect. This section will complement the theory of polarization error compensation through mathematical deduction.

The dual-polarization IFOG with a PMF coil and the dual-polarization IFOG with a depolarized coil are discussed in the previous two sections. They have the common point that two light waves of different polarization states are generated by the two-arm light path before the optical fiber coil. The experimental results show that the two polarization states are orthogonal, and the fiber delay line ensures that the two light beams are not coherent. At the same time, the two-arm light path can detect the two returned polarization states separately. The polarization evolution in this type of dual-polarization IFOG is shown in Fig. 2.7.

We use Jones Matrices to analyze the PN errors in the dual-polarization IFOGs. Common loss on two polarizations out of the coil is neglected, as they do not contribute to PN errors. Assuming that the degree of polarization (DOP) of the light source is d_0 , the field intensity thereof can be expressed as [5]

$$\mathbf{E}_0 = \begin{bmatrix} E_{0x}(t) \\ E_{0y}(t) \end{bmatrix} e^{j\omega_0 t} = \begin{bmatrix} \sqrt{1+d_0} \\ \sqrt{1-d_0} \end{bmatrix} E_0(t) e^{j\omega_0 t} \quad (2.1)$$

where ω_0 is light frequency, t is propagating time, DOP is $d_0 = (I_{0x} - I_{0y}) / (I_{0x} + I_{0y})$, and $-1 \leq d_0 \leq 1$. Thereafter, the two light waves are polarized to x and y directions respectively, and a delay length ΔL is added between them. This separate polarizing process can be represented by Jones matrices of two polarizers

$$\mathbf{P}_x = \begin{bmatrix} 1 & 0 \\ 0 & 0 \end{bmatrix} e^{-j\beta\Delta L}, \quad \mathbf{P}_y = \begin{bmatrix} 0 & 0 \\ 0 & 1 \end{bmatrix} \quad (2.2)$$

here β is propagation constant of the light wave. To correspond with the reference point in the later experiment, we define the point after the dual-polarization generation module as “Point C.” Then the light field of Point C is

$$\mathbf{E}_C = \alpha_1 \mathbf{P}_x \mathbf{E}_0 + \alpha_2 \mathbf{P}_y \mathbf{E}_0 = \begin{bmatrix} \alpha_1 \sqrt{1+d_0} e^{-j\beta\Delta L} \\ \alpha_2 \sqrt{1-d_0} \end{bmatrix} e^{j\omega_0 t} \quad (2.3)$$

here α_1 and α_2 are losses of two light signals, including splitting loss and transmitting loss. In order to clearly observe the law of dual-polarization light waves, we define the DOP of Point C as d , and normalize the light intensity, so that the light field of point C can be written as

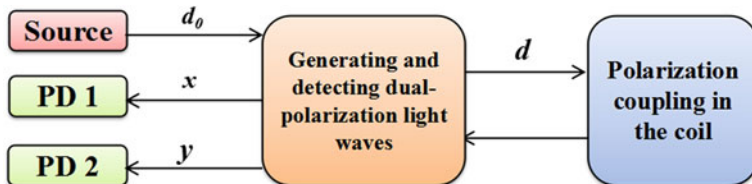


Fig. 2.7 The polarization evolution in the dual-polarization IFOG

$$\mathbf{E}_C = \begin{bmatrix} \sqrt{(1+d)/2} e^{-j\beta\Delta L} \\ \sqrt{(1-d)/2} \end{bmatrix} e^{j\omega_0 t} \quad (2.4)$$

There are two important differences between the polarization state of this light wave and the case of the “minimum scheme” ($|d| \approx 1$). One is $d \approx 0$, meaning the powers of the two polarization states are basically the same. The other is that a phase delay $e^{-j\beta\Delta L}$ is introduced between two polarizations for eliminating their coherence.

The random polarization coupling in the fiber coil is caused by a variety of reasons, including that the coil coupler, the phase modulator, and the fiber coil have nonideal polarization features. The CW light for instance, it undergoes coupler splitting, transmitting around the fiber loop, and recombining with the CCW light back to the coupler. The total polarization evolution of this period can be written as the following matrix.

$$\mathbf{M}_r^+ = \begin{bmatrix} C_{r1} & C_{r2} \\ C_{r3} & C_{r4} \end{bmatrix} \quad (2.5)$$

The superscript “+” means clockwise, the four items C_{r1} , C_{r2} , C_{r3} , C_{r4} in the matrix are complex numbers related to the polarization characteristics of the components. The subscript “r” indicates that the reciprocal ports are detected.

CW light and CCW light waves experience the same optical path, in the absence of external influences, and their transmission processes are reciprocal. When the interferometer rotates, the Sagnac effect introduces a nonreciprocal phase difference, but does not directly affect the polarization state. Ignoring the Faraday Effect for the time being, the polarization transfer matrix experienced by the CCW wave has a reciprocal form with the CW wave, that is, C_{r1} and C_{r4} remain unchanged, and the C_{r2} and C_{r3} positions are interchanged.

$$\mathbf{M}_r^- = \begin{bmatrix} C_{r1} & C_{r3} \\ C_{r2} & C_{r4} \end{bmatrix} \quad (2.6)$$

As transmission loss does not directly affect the PN error, the calculation for the time being does not consider the transmission loss of light in order to observe the polarization characteristics more clearly. In the ideal case without polarization coupling, the theoretical phase difference between the CW wave and the CCW wave after transmitting through the fiber loop is $\phi_r = \phi_S + \Delta\phi(t)$, in which $\Delta\phi(t)$ is the dynamic phase bias introduced by the phase modulator, and ϕ_S is the Sagnac phase shift. When there is polarization coupling in the optical path, the actual phase difference will deviate from the theoretical value due to the PN error, and the deviation degree of the two polarization states will be different. The phase difference caused by PN will be reflected in the result deduced by Jones matrix. The light component detected by the reciprocal port is calculated by the following equation, which includes a CW item and a CCW item.

$$\mathbf{E}_r^+ = \mathbf{M}_r^+ \mathbf{E}_C e^{j\phi_r}, \quad \mathbf{E}_r^- = \mathbf{M}_r^- \mathbf{E}_C \quad (2.7)$$

Their detailed expressions are derived as follows:

$$\mathbf{E}_r^+ = \begin{bmatrix} C_{r1} \sqrt{(1+d)/2} e^{-j\beta\Delta L} + C_{r2} \sqrt{(1-d)/2} \\ C_{r3} \sqrt{(1+d)/2} e^{-j\beta\Delta L} + C_{r4} \sqrt{(1-d)/2} \end{bmatrix} e^{j\omega_0 t} e^{j\phi_r} \quad (2.8)$$

$$\mathbf{E}_r^- = \begin{bmatrix} C_{r1} \sqrt{(1+d)/2} e^{-j\beta\Delta L} + C_{r3} \sqrt{(1-d)/2} \\ C_{r2} \sqrt{(1+d)/2} e^{-j\beta\Delta L} + C_{r4} \sqrt{(1-d)/2} \end{bmatrix} e^{j\omega_0 t} \quad (2.9)$$

CW and CCW waves interfere with each other, and generate the signal I_r for angular velocity detection

$$I_r = \langle |\mathbf{E}_r^+ + \mathbf{E}_r^-|^2 \rangle \quad (2.10)$$

Light intensities on two polarizations are detected separately by two PDs, so we calculate the intensities separately as follows:

$$\begin{aligned} I_{rx} &= \langle |\mathbf{E}_{rx}^+ + \mathbf{E}_{rx}^-|^2 \rangle \\ &= I_{rx0} + \langle \mathbf{E}_{rx}^+ * \mathbf{E}_{rx}^- \rangle + \langle \mathbf{E}_{rx}^- * \mathbf{E}_{rx}^+ \rangle \\ &= I_{rx0} + |C_{r1}|^2 (1+d) \cos \phi_r + (1-d) |C_{r2} C_{r3}| \Gamma(z_{r23}) \cos(\phi_r + \phi_{r23}) \end{aligned} \quad (2.11)$$

$$\begin{aligned} I_{ry} &= \langle |\mathbf{E}_{ry}^+ + \mathbf{E}_{ry}^-|^2 \rangle \\ &= I_{ry0} + \langle \mathbf{E}_{ry}^+ * \mathbf{E}_{ry}^- \rangle + \langle \mathbf{E}_{ry}^- * \mathbf{E}_{ry}^+ \rangle \\ &= I_{ry0} + |C_{r4}|^2 (1-d) \cos \phi_r + (1+d) |C_{r2} C_{r3}| \Gamma(z_{r23}) \cos(\phi_r - \phi_{r23}) \end{aligned} \quad (2.12)$$

here I_{rx0} and I_{ry0} are the direct-current components that have no direct influence on the detection signal, $\Gamma(z)$ is the source's degree of coherence [6], z_{rij} is the birefringence delay induced by $C_{ri} C_{rj}^*$, and ϕ_{rij} is the phase of $C_{ri} C_{rj}^*$, with $i, j \in \{1, 2, 3, 4\}$. In this calculation, it is assumed that the decoherence effect is ideal, that is, the coherence is ignored between the light waves whose phase difference is larger than $\beta\Delta L$. Thus, the corresponding weakly coherent terms have been omitted from the results obtained.

It can be observed from the last terms of (2.11) and (2.12) that the theoretical value of the signal ϕ_r have opposite deviations for x and y polarizations, given by $+\phi_{r23}$ and $-\phi_{r23}$. In order to analyze the inverse feature of the test results more clearly, the signals are further written in the following forms.

$$I_{rx} = I_{rx0} + q_{rx} \cos \phi_r + p_{rx} \sin \phi_r = I_{rx0} + \sqrt{p_{rx}^2 + q_{rx}^2} \cos(\phi_r - \Delta\phi_{rx}) \quad (2.13)$$

$$I_{ry} = I_{ry0} + q_{ry} \cos \phi_r + p_{ry} \sin \phi_r = I_{ry0} + \sqrt{p_{ry}^2 + q_{ry}^2} \cos(\phi_r - \Delta\phi_{ry}) \quad (2.14)$$

where p_{rx} , q_{rx} , p_{ry} , q_{ry} are intermediate parameters introduced for convenient analysis. And $\Delta\phi_{rx} = \arctan(p_{rx}/q_{rx})$ and $\Delta\phi_{ry} = \arctan(p_{ry}/q_{ry})$ are PN errors in the x and y polarizations, respectively. The results of the two signals are summed up as follows:

$$I_r = I_{rx} + I_{ry} = I_{r0} + \sqrt{(p_{rx} + p_{ry})^2 + (q_{rx} + q_{ry})^2} \cos(\phi_r - \Delta\phi_r) \quad (2.15)$$

where I_{r0} is the sum of the DC components in the sum signal, and the PN error is transformed into

$$\Delta\phi_r = \arctan \frac{p_{rx} + p_{ry}}{q_{rx} + q_{ry}} \quad (2.16)$$

By transforming formulas (2.11) and (2.12) to formulas (2.13) and (2.14), the related parameters and the PN errors are derived as follows:

$$p_{rx} = -(1-d)|C_{r2}C_{r3}|\Gamma(z_{r23}) \sin \phi_{r23} \quad (2.17)$$

$$p_{ry} = (1+d)|C_{r2}C_{r3}|\Gamma(z_{r23}) \sin \phi_{r23} \quad (2.18)$$

$$q_{rx} = |C_{r1}|^2(1+d) + (1-d)|C_{r2}C_{r3}|\Gamma(z_{r23}) \cos \phi_{r23} \quad (2.19)$$

$$q_{ry} = (1-d)|C_{r4}|^2 + (1+d)|C_{r2}C_{r3}|\Gamma(z_{r23}) \cos \phi_{r23} \quad (2.20)$$

$$\Delta\phi_r = \arctan \frac{2d|C_{r2}C_{r3}|\Gamma(z_{r23}) \sin \phi_{r23}}{|C_{r1}|^2(1+d) + |C_{r4}|^2(1-d) + 2|C_{r2}C_{r3}|\Gamma(z_{r23}) \cos \phi_{r23}} \quad (2.21)$$

where $\Gamma(z)$ is the source's degree of coherence, z_{rij} is the birefringence delay induced by $C_{ri}C_{rj}^*$, and ϕ_{rij} is the phase of $C_{ri}C_{rj}^*$, with $i, j \in \{1, 2, 3, 4\}$.

The calculation results show that p_{rx} and p_{ry} have opposite signs, which also indicate that PN errors on two signals $\Delta\phi_{rx}$ and $\Delta\phi_{ry}$ have opposite signs, so they can compensate each other by mutual superimposition. When the dual-polarization light is generated by uniform light splitting, we have $d = 0$ and thus $p_{rx} = p_{ry}$. In this case, the numerator in (2.16) is zero, $p_{rx} + p_{ry} = 0$. Hence PN signals are perfectly compensated after the superimposition $\Delta\phi_r = 0$.

The numerically calculated results for the intermediate parameters $p_{rx,y}$ and $q_{rx,y}$ are shown by Fig. 2.8, with the DOP d scanned in its whole possible range $[-1, 1]$. It can be seen that p_{rx} and p_{ry} have opposite signs in the whole range. When $d = 0$, the compensated parameter $p_r = p_{rx} + p_{ry}$ just crosses the zero point, as shown by

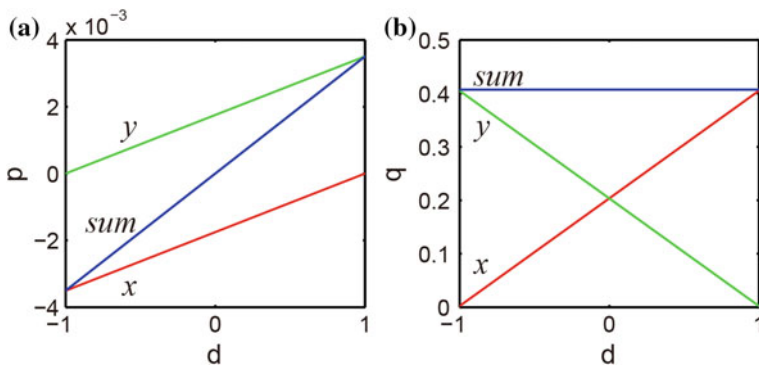


Fig. 2.8 The variation of p , q with d in the compensation formula **a** p varies with d , **b** q varies with d

sum in Subgraph (a). q_{rx} and q_{ry} have a roughly complementary trend, and thus $q_r = q_{rx} + q_{ry}$ is a stable nonzero number, as shown by sum in Subgraph (b). According to the parameter definition $\Delta\phi_r = \arctan(p_r/q_r)$, it can be seen that the variation tendency of the error is almost the same as that of the parameter p_r , and it will be compensated to zero when $d = 0$.

This theoretical analysis based on the Jones matrix shows that the PN errors for the two polarization states x , y have opposite signs. This also explains the reason for the inverse noises on the two signals detected in experiment. By summing up the light intensities of the two polarizations, or by summing up the obtained photocurrent signals at the PD, the PN errors can be compensated and thus eliminated. This superimposition process is just the PN error compensation mechanism in the dual-polarization IFOG. The derivation of the formulas also shows the two conditions required for PN error compensation: one is that the two polarization states need balanced power, that is, $d = 0$; the other is that the coherence needs to be eliminated between the two polarizations by a propagation delay. When both conditions are satisfied, it is theoretically possible to completely eliminate the PN error by compensation.

2.4 Summary

In this chapter, we first analyze two experiments, including a dual-polarization IFOG based on a PMF coil, and a dual-polarization IFOG based on a depolarized SMF coil. In both experiments, polarization error compensation is observed. The error components with opposite signs exist in the two polarization states, which can be eliminated by superimposition. This part of the error component is mainly caused by the PN error introduced by polarization coupling.

Thereafter, the Jones matrix is used to analyze the error compensation phenomena in the dual-polarization IFOG, and the conditions of PN error compensation are proved. The analysis shows that when the two polarization states have balanced power and no coherence, the PN errors within the two signals are opposite, and can be completely compensated by superimposition. Obviously, obtaining a DOP $d = 0$ is the basic requirement for the dual-polarization IFOG to work stably. In the next chapter, we will design and validate a more compact and practical dual-polarization IFOG, based on the basic conclusions in this chapter.

In addition, the fundamental principles of polarization error compensation demonstrated in this chapter also provide the basis for multiple optical compensation and Shupe error compensation in IFOGs [7–9].

References

1. Y. Yang, Z. Wang, Z. Li, Optically compensated dual-polarization interferometric fiber-optic gyroscope. *Opt. Lett.* **37**, 2841–2843 (2012)
2. G. Zhang, *The Principles and Technologies of Fiber-Optic Gyroscope*, (National Defense Industry Press, 2008)
3. F.L. Walls, D.W. Allan. Measurements of frequency stability. *Proc. IEEE* **74**, 162–168 (1986)
4. IEEE Standard specification format guide and test procedure for single-axis interferometric fiber optic gyros. IEEE Std 952–1997 (2008R)
5. G.A. Pavlath, H.J. Shaw, Birefringence and polarization effects in fiber gyroscopes. *Appl. Optics*. **21**, 1752–1757 (1982)
6. B. Szafraniec, G.A. Sanders, Theory of polarization evolution in interferometric fiber-optic depolarized gyros. *J. Lightwave Technol.* **17**, 579–590 (1999)
7. P. Lu, Z. Wang, Y. Yang, D. Zhao, S. Xiong, Y. Li, C. Peng, Z. Li, Multiple optical compensation in interferometric fiber-optic gyroscope for polarization nonreciprocal error suppression. *IEEE Photon. J.* **6**, 7200608 (2014)
8. P. Lu, Z. Wang, R. Luo, D. Zhao, C. Peng, Z. Li, Polarization nonreciprocity suppression of dual-polarization fiber-optic gyroscope under temperature variation. *Opt. Lett.* **40**, 1826–1829 (2014)
9. X. Xua, F. Teng, Z. Zhang, C. Zhang, N. Song, Analysis and simulation of a fiber optical gyroscope with Shupe error compensated optically. *J. Mod. Opt.* **61**, 931–937 (2014)

Dual-Polarization Two-Port Fiber-Optic Gyroscope

Wang, Z.

2017, XVI, 93 p. 60 illus., 54 illus. in color., Hardcover

ISBN: 978-981-10-2835-9